Case Studies in Construction Materials 20 (2024) e03129

Contents lists available at ScienceDirect

Case Studies in Construction Materials

journal homepage: www.elsevier.com/locate/cscm

A comparative study on the seismic performance of long span Engineered Cementitious Composite (ECC) structures

Sikandar Ali Khokhar [a,b], Shahzeb Memon [a], Touqeer Ahmed [a,b], Muhammad Umer Basit [a], Fawad Ahmed Najam [a,c], Rao Arsalan Khushnood [a,d,*]

[a] NUST Institute of Civil Engineering (NICE), School of Civil and Environmental Engineering (SCEE), National University of Sciences and Technology (NUST), Sector H-12, Islamabad 44000, Pakistan
[b] Bendcrete Construction Services (Pvt) Ltd., National Science and Technology Park (NSTP), Sector H-12, Islamabad 44000, Pakistan
[c] School of Engineering, Faculty of Applied Science, University of British Columbia, Okanagan, Canada
[d] Department of Structural, Geotechnical and Building Engineering, Politecnico di Torino, Corso Duca degli Abruzzi 24, Turin 10129, Italy

ARTICLE INFO

Keywords:
Long-span buildings
Engineered cementitious composite
Nonlinear analysis
Seismic performance
Finite element modeling

ABSTRACT

The strain hardening fiber reinforced concrete—generally known as the Engineered Cementitious Composite (ECC)—has rapidly gained the attention of researchers in recent years. However, most of the research on ECC is limited to material and member level, leaving a gap in the understanding of its behavior at the structural scale. Therefore, this study investigates the global seismic response of ECC structures and compares their performance with conventional reinforced concrete (RC) structures. For this purpose, a case study long span building structure (an aircraft hangar having a span length of 40 m) is selected. Under the design-level gravity and lateral loads, its members are separately designed using the conventional RC and ECC. It is observed that for ECC members, the requirement of longitudinal steel is reduced by 30% when compared with the conventional RC members. Similarly, owing to an improved tensile behavior, the ECC members also exhibited a higher shear capacity than RC members, resulting in a significant reduction in the requirement of transverse reinforcement. The detailed inelastic finite element models for both design cases (RC and ECC) were subjected to the pushover analysis and nonlinear response history analysis (NLRHA) to assess their seismic performance. It is observed that (in terms of local and global seismic demands, structural damage, and ductile behavior) the performance of the ECC structure is significantly improved when compared to the conventional RC structure. The comparative cost analysis showed a reduction of 11.9% in the overall material cost of the ECC structure as compared to RC. These results show that ECC can be effectively used at the full structural level as an economic solution to ensure the ductile response and superior seismic performance.

Abbreviations: ECC, Engineered Cementitious Composites; FRC, Fiber Reinforced Concrete; FEM, Finite Element Modeling; ACI, American Concrete Institute; JSCE, Japan Society of Civil Engineers; NLRHA, Nonlinear Response History Analysis; ISMD, Integrated Structures and Materials Design; ML, Machine learning; ETABS, Extended Tabular Analysis and Design of Building Structures; RC, Reinforced Concrete.

* Corresponding author at: NUST Institute of Civil Engineering (NICE), School of Civil and Environmental Engineering (SCEE), National University of Sciences and Technology (NUST), Sector H-12, Islamabad 44000, Pakistan.
E-mail address: arsalan.khushnood@nice.nust.edu.pk (R.A. Khushnood).

https://doi.org/10.1016/j.cscm.2024.e03129
Received 10 June 2023; Received in revised form 17 November 2023; Accepted 3 April 2024
Available online 4 April 2024

1. Introduction

The structural design of long-span concrete structures is extremely challenging for designers. This is mostly owing to high moment demands, which cause undesired high tensile stresses [1] and most of the construction materials except steel are weak in tension. Despite the complexity involved in their design, they are very popular commercially. Their popularity derives from their necessity in numerous special applications such as industrial sheds, aircraft hangars, halls, auditoriums, etc. Additionally, long-span structures may assist in cutting off the cost of intermediate supports, resulting in a more economical design. In the early 10th century, these high demands were resisted by the use of arches and domes, which reduced the flexural stresses and produced axial compressive stresses [2]. Later in the 1940 s, reinforced concrete (RC) was proposed for medium to long-span structures incorporating an excessive amount of steel reinforcement [3]. Furthermore, the advancements in construction materials helped structural engineers to design cost effective infrastructures. In this way, pre-stressed concrete was introduced for long-span structures, eliminating high reinforcement and cross-sectional requirements. However, prestressed concrete possesses a shortcoming related to its ductility [4,5]. This limitation becomes a critical concern when the structure lies in a seismically active region, as seismic design codes recommend the structure and its elements to be ductile in high seismic zones [6]. Therefore, RC with an excessive amount of steel reinforcement becomes a compulsion in seismic regions to ensure adequate confinement for ductility [4,5]. However, RC makes the design uneconomical due to high reinforcement requirements. So, there is a need for an innovative material that can provide ductility without any compromise on cost, to ensure resilient and cost effective infrastructures.

Several innovative solutions have been proposed to improve the seismic performance of structures by providing ductile elements and links [7,8]. One of these is to introduce fibers in the cementitious matrix to make the composite ductile. These composites are termed as fiber reinforced concrete (FRC) [9,10–12]. A special class of high performance FRC that exhibits strain-hardening behavior in uniaxial tension is classified as Engineered Cementitious Composite (ECC) [13–15] [16–18]. ECC can be a potential candidate to reduce cross sections and reinforcement requirements due to its enhanced tensile capacity as compared to conventional concrete[19]. Additionally, ECC is lightweight and highly ductile which may also help to improve the seismic performance of the structure [20–25, 26]. However, its material processing and design is not as simple as that of conventional concrete [27], as it requires a micro-mechanical model to obtain a mix that will ensure strain hardening response. To study its structural behavior, its material properties are incorporated by the integrated structures and materials design (ISMD) approach proposed by Li [28]. ISMD specifies that material design should be carried out first to obtain the necessary constitutive model for structural analysis and design.

Several studies have been conducted on different aspects of ECC to study its behavior at the member level using the ISMD [15]. Li et al. [29] reported that due to the inherent ductility of ECC, it performs better under cyclic loadings as compared to conventional concrete. ECC has also been proven to possess a high load carrying capacity [30], which is necessary for long-span structures. Maalej and Li [31] and Szerszen et al. [32] studied the behavior of reinforced ECC members subjected to flexural stresses and developed a moment-curvature relationship for steel reinforced ECC beams. Similarly, Ding et al. [33] studied the structural behavior of ECC beams and concluded that the load bearing capacity of non-steel reinforced ECC beams was equivalent to the RC beams with a reinforcement ratio of 1.86%. Similarly, the behavior of columns, shear walls, and beam-column connections was studied under different types of static and dynamic excitations [34,35–39]. Due to its enhanced mechanical properties, it was also recommended for the repair and retrofitting of damaged and deficient RC members [40–45]. However, most of the studies related to ECC are limited to member and material levels with no comprehensive performance based assessment carried out on a complete structural scale. So, in order to compare the seismic response of ECC and RC, a complete structural level study is needed on a long-span structure subjected to realistic loadings using detailed performance-based design/assessment procedures.

This study focuses on the structural design and performance based seismic assessment of long-span ECC structures. Initially, the material design was performed following the ISMD approach [15] to obtain material properties using a simplified machine learning based approach [46]. A case study structure having a span of 40 m was selected for finite element modeling. A Finite element model (FEM) of ECC on a complete structural scale was developed for the case study structure. For the comparative study, an RC finite element model with the same case study structure was also developed. The linear static analysis method was adopted to obtain local design actions against dead, live, and seismic loads. For the elastic design, JSCE [47] guidelines were used for ECC, while ACI 318–19 [48] was employed for RC design. The design results revealed that the reinforcement requirements for ECC were significantly lower and impractical. The practical approach would be to use a reduced cross-section model for ECC. Therefore, the third model with reduced cross sections of ECC was also considered for comparative analysis. To simulate the actual behavior of ECC, nonlinear modeling and analyses were conducted to capture its actual response. For performance based evaluation, nonlinearity was induced only in frame elements, while slabs were modeled as linear elastic. For beams, plastic hinges were assigned using moment rotation curves as per ASCE 41–17 [49], while the fiber modeling technique was employed for columns. Nonlinear response history analysis (NLRHA) and pushover analysis were performed to assess the local and global seismic demands and to simulate the actual response of the structure. Finally, the economic potential of ECC is investigated through material cost estimation and cost comparison with RC.

2. Development of ECC mix

Usually, the material and structural design are performed by two distinct parties and the only connection between the two is the compressive strength of concrete, regardless of the sequence of design. This method is inapplicable to ECC as its constitutive model cannot be generated until the material design is finalized. The Integrated Structures and Materials Design (ISMD) method proposed by Li [15] enables the structural performance to be linked with ECC constituent selection and tailoring. For the usefulness of the ISMD [15] approach, a constitutive model is needed that when combined with the finite element method, should represent the material

properties on the structural scale. Therefore, the structural design of ECC should be performed after finalizing the material design and obtaining the constitutive model. ISMD approach linking structural performance to material properties is shown in Fig. 1.

It is extremely challenging to proportionate a mix that exhibits strain hardening response which makes the material design of ECC quite complex [10–12]. Initially, it was assumed that strain hardening could only be achieved by increasing the fiber content, however, this does not appear to be a viable alternative due to the high cost and difficulties associated with the workability of the mix. Later research suggested that fiber content is not the only factor influencing this behavior [50,51]. The other important parameters that could influence the behavior of FRC in tension include matrix toughness, matrix tensile strength, fiber properties (elastic modulus, yield strength, aspect ratio, etc.), and matrix-fiber interfacial properties (frictional bond, snubbing coefficient, etc.) [52,53]. Numerous researchers [51–57] have presented various approaches for estimating the critical volume fraction (minimum volume of fibers required for strain hardening), by establishing the correlations among the above-mentioned parameters.

The ECC mix design method is based on a micro-mechanical model (commonly used model for calculating critical volume fraction of fibers) that necessitates a series of experiments, making the design process extensive, time-consuming, and costly [58]. Consequently, a relatively novel technique, based on a machine learning (ML) model, is applied for obtaining a required mix design [25]. The machine learning based model was utilized to determine the ECC mix of 35 MPa as well as its associated tensile strength and strain [25]. Table 1 displays the ECC mix calculated using the ML method [25], which was employed for the design. Table 1 also displays the fiber properties and output parameters predicted by the ML model. As PVA fibers are mostly used in ECC, therefore a mix with PVA fibers was used.

3. Selection and design of a case study long-span structure

The selected case study structure is an aircraft hangar located in Karachi, Sindh, Pakistan. The hangar has dimensions of 56 m by 56 m with a clear span of 40 m by 40 m. The plan of the hangar with the beam and column locations is elaborated in Fig. 2. The hangar is an intermediate moment resisting framed structure without any shear walls or core walls. The gravity loads are carried by slabs and beams which rest on columns. A curved waffle slab covers the entire aircraft parking space. Fig. 2 shows the plans, elevations, and 3D model of the case study structure while Table 2 shows the architectural details of the case study structure.

A comprehensive study is conducted to evaluate the seismic performance of ECC as compared to RC. For the analysis and design, two finite element models (FEM) are developed to compare the structural performance of the novel composite. For the sake of initial analyses, and to obtain design actions linear static analysis procedure was performed. For the analysis, the input properties for both the composites (ECC and RC) were separately incorporated into the respective models. Table 3 shows the input material properties considered for the analysis and design of the structures.

Similar sorts of loads were applied to both computer models. The specifications of seismic and live loads for both models were kept constant. However, the dead load was different due to the difference in unit weight of ECC and RC. The seismic coefficients are selected according to the building code of Pakistan 2021 (BCP-2021) [59]. The numerical values of the loading patterns and specification of seismic loading are summarized in Table 4.

The linear static analysis is performed for both models, for which loads (dead load, live load, and seismic load) and their combinations are selected according to ASCE 7–16 [60]. The mass source was defined for the structure as the sum of the dead load and 25% of the live load as per the International Building Code (IBC) 2021 [6]. The analysis is performed by modeling seismic load as equivalent lateral force (ELF) procedure following the procedure of ASCE 7–16 [38]. For analyses, the meshing was provided in a rectangular pattern at a distance of 0.33 m. The slabs were modeled as thin shell elements and a rigid diaphragm was assigned to restrict the relative movement within the slabs. The second order analysis was also incorporated using a non-iterative P delta technique based on mass.

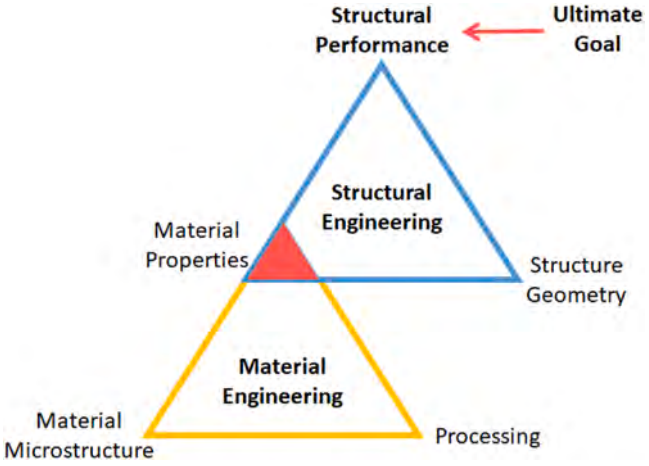

Fig. 1. ISMD [15] approach linking structural performance with composite's material properties.

Table 1
Selected mix of ECC sample, Properties of fibers, and Output parameters of ML model.

		Selected mix of ECC		
Cement	Fly ash	Sand	W/B	HRWR*
1	0.6	0.6	0.55	0.6%
		Properties of Fiber		
Volume fraction	Elastic modulus	Length	Diameter	
2%	40 GPa	12 mm	40 μm	
		Output parameters of ML model		
Compressive Strength	Tensile Strength	Tensile Strain	Post Cracking Response	
35.2 MPa	4.7	3.7%	Strain-hardening	

*High range water reducer (Polycarboxylate ether based)

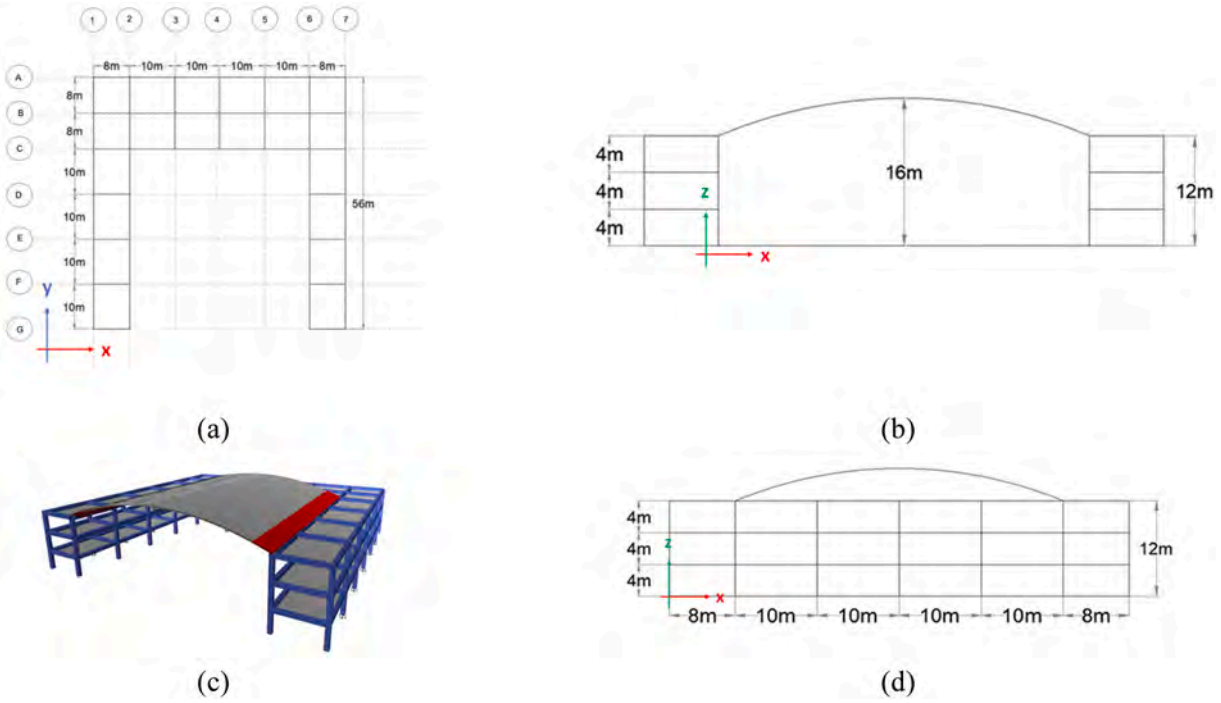

Fig. 2. Architectural models of the case study structure (a) floor plan (b) front elevation (c) 3D model (d) back elevation.

Table 2
Architectural details of the case study structure.

Details	Dimensions
Number of Stories	3
Total Height of Office spaces	12 m
Total Height of the Parking Space	16.1 m
Typical Story Height	4 m
Floor Area	56 m x 56 m
Span	40 m

The effect of cracked concrete on stiffness was accounted for by the concrete stiffness modifiers as per provisions of ACI 318–19 [27]. However, for ECC stiffness modifiers are expected to be approximately double as compared to that of RC [26], but as they were not numerically available so being on the conservative side same stiffness modifiers were used for both models.

The static analysis revealed that the design actions for ECC members were considerably lower due to the lower unit weight of the composite which suppressed dead and seismic loads. The comparison of member responses in terms of shear force and bending moments for some of the specified beams and columns are graphically shown in Figs. 3 and 4.

The next phase, following the analysis, was to design the structural members. The structural design of RC was performed directly with the aid of ACI 318–19 code [27]. As ECC possesses significant tensile strength that needs to be considered for the structural design. ACI 318–19 [27] ignores the tensile capacity of concrete hence it cannot be used for the structural design of ECC. Therefore, the elastic

Table 3
Input material properties.

Specifications	Conventional concrete	ECC	Steel Rebar
Compressive Strength	35 MPa	35 MPa	420 MPa
Tensile Strength	-	4.8 MPa	420 MPa
Elastic Modulus	27.8 GPa [26]	14.8 GPa	210 GPa
Poisson's ratio	0.2 [26]	0.226	0.28
Tensile strain Capacity	-	3.7%	10.8%
Unit weight	2400 kg/m^3	1800 kg/m^3	7850 Kg/m^3

Table 4
Loads along with their specifications used for the design of case study structure.

Load pattern	Factors	Value
Dead load	-	As per unit weight
Live load	-	1 KN/m^2
Seismic Load	S_s	0.94 g
	S_1	0.30 g
	Site class	D
	Long period transition period	8 sec
	Response modification factor	5
	System overstrength factor	3
	Deflection amplification	5.5
	Occupancy importance factor	1

design of ECC was performed using the Japan society of civil engineering (JSCE) guidelines "Recommendations for design and construction of high-performance fiber reinforced concrete with multiple fine cracks" [26]. JSCE guidelines provide a simplified stress and strain distribution for both compression and tension stresses along the depth for flexural members as shown in Fig. 5. Longitudinal reinforcements for beams and slabs are computed against design bending moments calculated via linear static analyses. Alongside, special attention was given to beam to column capacity ratio to ensure that the column yields first as prescribed by the seismic design codes [6,27].

Furthermore, in reinforced ECC a major proportion of shear is resisted by fibers that must be incorporated in shear design. JSCE guidelines [26] provide a simplified equation to calculate the shear capacity of the ECC members by using Eqs. (1) and (2). It can be seen that mainly three components are providing shear resistance for ECC. The additional parameter is the shear resisted by the fibers which is not present for conventional RC.

For column design, three-dimensional capacity interaction surfaces were used. These capacity surfaces were developed using the nonlinear fiber modeling approach. Reinforcements are assumed and trial cross-sections are employed in ascending order. The design actions and the three-dimensional capacity surface are compared to calculate adequate cross-section and optimum amount of steel for ECC columns.

$$V_u = V_c + V_s + V_f \tag{1}$$

Where V_s, V_s, and V_f are the shear capacities provided by concrete, transverse steel, and fibers respectively. While V_u is the ultimate shear capacity of the member.

$$V_f = \left(\frac{f_{vd}}{\tan(\beta_u)}\right).b_w.\frac{z}{\gamma_b} \tag{2}$$

f_{vd} design tensile yield strength of ECC, $f_{vd} = 0$ when f_{vd} is smaller than 1.5 N/mm^2.
β_u angle of the diagonal crack surface to the member axis. $\beta_u = 45^0$.
γ_b 1.3 for shear (Factor of safety)
z distance between location of compressive stress resultant to centroid of tensile steel, may generally use d/1.15.

Tables 5 and 6 with Fig. 6 show the comparison of reinforcement requirements of both models. It is clear that the reinforcement needed in ECC members is comparatively lower than in RC and is mostly governed by the minimum reinforcement requirements. It suggests that the cross sections for the ECC model should be further reduced to get a more economical and practical design. Therefore, a third model was developed with reduced cross sections, and its analyses and design were performed in a similar manner. Its static analysis showed an average of 20% further reduction in the design actions, due to the lower self-weight of the elements. The design results of the reduced cross-sections ECC model are summarized in Table 7.

The design results, as shown in Tables 5, 6, and 7, show that the reinforcement requirement for ECC models was considerably lower as compared to RC. It is mainly due to the lower unit weight of ECC (which suppressed the dead and seismic load), and the promising tensile capacity of ECC. Further reduction in cross section led to more reduced demands resulting in a more economical design.

The design performed as per JSCE guidelines [26] showed an average of 30% reduction in the longitudinal steel requirements along with a 25% reduction in cross-section for beams. Similar results were obtained by Szerszen et al. [19] while studying ECC members and

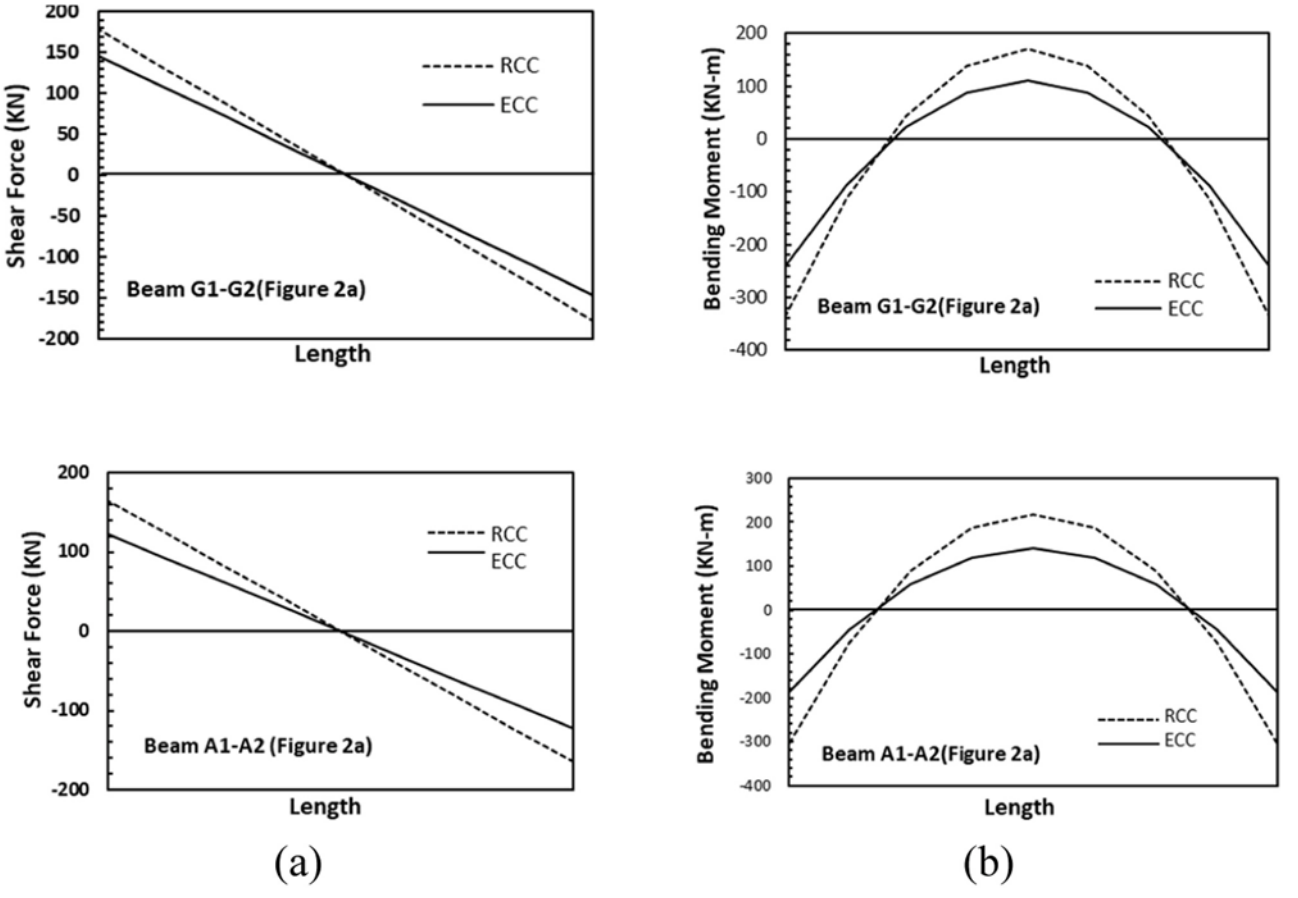

Fig. 3. (a) Comparison of shear forces in 3rd storey beams along the length, (b) Comparison of bending moments in beams in 3rd storey along the length (Refer Fig. 2 for G1-G2 and A1-A2).

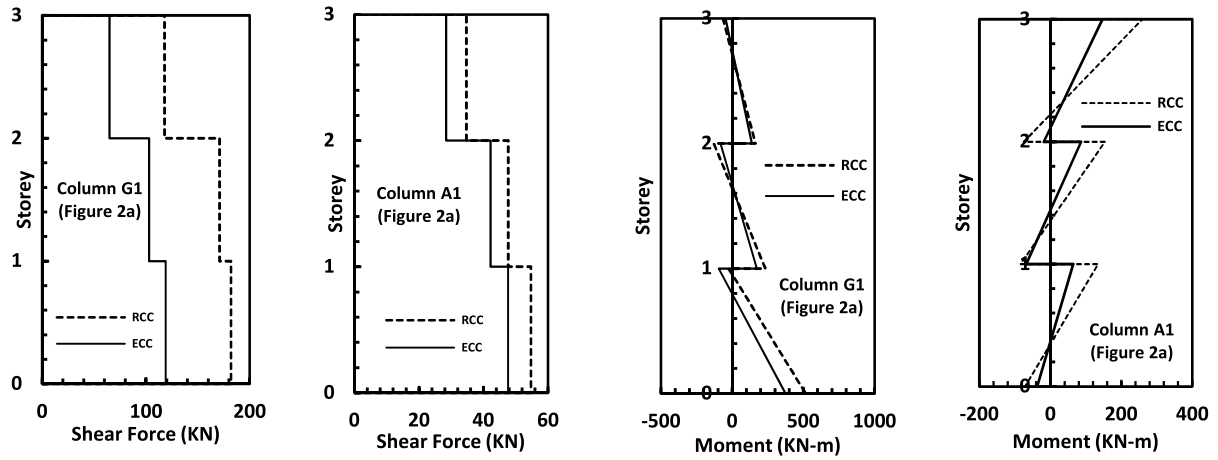

Fig. 4. The distribution of shear force and moment along the height in specified columns (Refer Fig. 2 for A1 and G1).

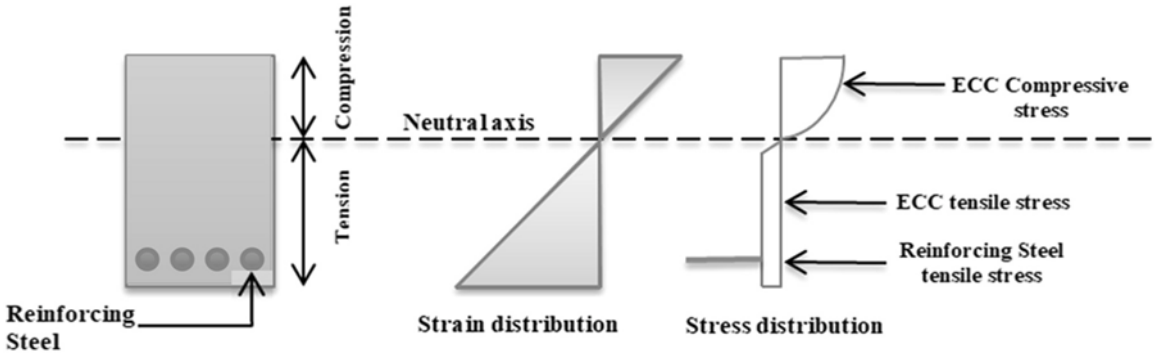

Fig. 5. Flexural stress & strain profile as per JSCE guideline.

Table 5
Design results for beams.

Beams	ECC				RC		
	Size (BxH) mm	Longitudinal Reinforcement		Shear reinforcement	Longitudinal Reinforcement		Shear reinforcement
		Top	Bottom		Top	Bottom	
Exterior beams	500 ×600	3 # 22 bars	3#10 bars	-	4 # 32 bars	3 # 25 bars	#13 @ 100 mm c/c
Interior beams	500×600	3#19 bars	3#10 bars	-	2 #32 bars	2 # 22 bars	#13 @ 115 mm c/c
Middle beams	600 ×700	3# 25 bars	3#10 bars	-	2 #32 bars	2 # 22 bars	#13 @ 100 mm c/c

Table 6
Design results of columns.

Columns	RC			ECC		
	Size (BxH) mm	longitudinal steel (mm^2)	Shear reinforcement	Size (BxH) mm	longitudinal steel (mm^2)	Shear reinforcement
Exterior Columns	600 ×600	2036	#13 @ 100 mm c/c	600 ×600	1620	-
Interior Columns	600 ×600	14000	#13 @ 50 mm c/c	600 ×600	12900	-
Middle Columns	600 ×600	3600	#13 @ 130 mm c/c	600 ×600	3600	-

reported an increase in capacity by up to 230% for smaller values of reinforcement with similar cross sections. Likewise, Ding et al. [33] studied the structural response of ECC beams and concluded that the moment capacity of non-steel reinforced ECC beams was comparable to the RC beams. Moreover, owing to an improved tensile behavior, the ECC members also exhibited a higher shear capacity than RC members, as a result theoretically no shear reinforcement was required in the complete structure. Li et al. [61] also reported that the shear capacity of ECC beams without stirrups is comparable to RC beams with adequate shear reinforcement provided

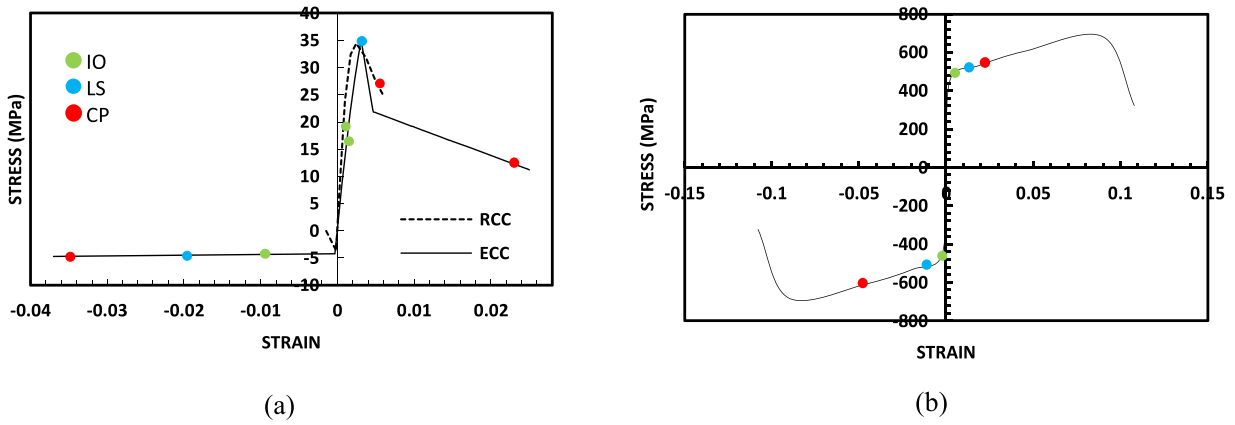

Fig. 6. Stress-strain curves (a) for ECC and Conventional concrete (b)Steel Rebar.

Table 7
Design results of ECC Reduced cross section model.

Beams	Beams				Columns	Columns		
	Size (BxH) mm	Longitudinal Reinforcement		Shear reinforcement		Size (BxH) mm	longitudinal steel (mm^2)	Shear reinforcement
		Top	Bottom					
Exterior beams	250 ×500	3 # 25 bars	2 # 22 bars	-	Exterior columns	600 ×600	1748	-
Interior beams	250 ×500	2 # 25 bars	2 # 19 bars	-	Interior columns	600 ×600	13900	-
Middle beams	250 ×500	3 #29 bars	3 # 22 bars	-	Middle columns	450 ×450	4072	-

using the Ohno shear test. The same was also reported by Shimizu et al. [62] while studying reinforced PVA-ECC beams. The enhanced shear capacity is mainly due to fiber bridging and micro cracking phenomena. These previous studies also validate that the ECC member without any shear reinforcement is also safe [39,40,63,64]. The design results of columns are also improved as compared to RC. The overall requirement for longitudinal steel is reduced up to 15% with no requirement for transverse reinforcement. The performance of reinforced ECC columns has been experimentally investigated when subjected to cyclic loadings [20]. The study showed an increased capacity of reinforced ECC columns as compared to RC columns. RC column showed severe cracks of width reaching 2.5 mm at 0.015 rad deflection angle. While those in reinforced ECC are only 0.3 mm at 0.03 rad deflection angle [20]. This study also validates the improved performance of ECC columns numerically on the complete structural level.

Furthermore, the eigenvalue analysis was performed to evaluate the modal properties and natural time periods of the structure. The modal analysis showed a linear translation along the principal axis in the first two modes and showed torsional deformation in the third mode which removes the concerns related to any eccentricity within the structure. Table 8. shows the summary of modal analysis results. It can be observed that the natural time periods for the ECC models are relatively higher due to lower structural level stiffness, which can be the result of lower modulus of elasticity, reduced cross-sections, and lower stiffness modifiers assumed for the ECC model. Since for ECC, the cracks are bridged by the fibers, the damage tolerance of ECC translates into enhancement in the tension stiffening response of reinforced ECC members. In general, tension-stiffening is defined as the increase in stiffness over the bare steel reinforcement due to the tensile load carried by the concrete material after cracking [65,66]. It is estimated that the stiffness modifiers should be double as those for RC [26]. However, due to the unavailability of numeric values of the stiffness modifiers for ECC, being on the conservative side, the same stiffness modifiers are used for both materials.

Table 8
Modal analysis result summary.

Time Period	ECC (Reduced Cross-section) sec	ECC (same sections) sec	RC sec
1st Mode (Translation in X)	1.905	1.795	1.057
2nd Mode (Translation in Y)	1.869	1.683	0.97
3rd Mode (Torsional)	1.699	1.543	0.882

4. Performance based seismic evaluation

The structural failures due to seismic activities have revealed the uncertainties of code based design procedures and demonstrated the necessity of methodologies for structural performance evaluation and design. The root cause of the problem is the insufficient assessment and treatment of the substantial uncertainties in the loadings and the complex structural behavior in the nonlinear range [67]. Performance based analysis allows us to capture the complete material behavior, even beyond the linear elastic range. Since ECC exhibits good post-cracking response, nonlinear analyses are required to fully capture its response at the structural level, which cannot be done using linear analysis. In addition to that, there may be uncertainties involved with new and novel material like ECC, these can be accounted for by performance based assessment.

For this study, a comparative performance based seismic evaluation of both the composite materials (RC and ECC) is carried out using pushover analysis (nonlinear static) and non-linear response history analysis (nonlinear dynamic) against both design basis earthquake (DBE) and maximum considered earthquake (MCE). DBE-level earthquake is defined as a ground motion having a 10% probability of exceedance in 50 years whereas MCE-Level earthquake is defined as a ground motion having a 2% exceedance in 50 years. Furthermore, to assess the seismic performance of ECC, the results from the nonlinear analysis of the conventional concrete model are compared with 2 different ECC models, one having the same cross-sections as the conventional concrete model and the other with reduced cross-sections, as discussed in Section 3. In short, there are a total of 3 inelastic models, and all 3 models are analyzed for both DBE and MCE level earthquakes yielding a total of 6 seismic responses.

4.1. Nonlinear modeling

For the purpose of performing detailed Nonlinear Response History Analysis (NLRHA) and Pushover Analysis (PA), nonlinear 3D models are created using ETABS [68]. Beams and columns are modeled as nonlinear elements whereas slabs are modeled as linear elastic. To introduce nonlinearity in beams, moment rotation plastic hinges are modeled as per ASCE-41–17 [69] provisions. These plastic hinges are modeled at 0.1 L distance from the beam ends (L being the beam span). The shear behavior is assumed to be linearly elastic, but shear demands are checked and compared against corresponding capacities to check for any shear failure. For columns nonlinear fiber modeling approach is used to capture the nonlinear behavior of columns. In this approach, the cross-section of the element is divided into a specific number of fibers, with some fibers made up of concrete, and some of the embedded steel rebars, and each fiber is then assigned the respective stress strain model. In all 3 nonlinear models, fibers are assigned up to the length of 0.1 at both ends of the columns. A constant modal damping is defined as 5% for all the modes in all three FEMs.

The material level constitutive models for steel, conventional concrete, and ECC are assigned to the respective models along with their hinge limits as shown in Fig. 6. For steel, Park's model, and for conventional concrete Mander's model [70] is used to obtain the idealized stress strain relationship. The mathematical formulation of Mander's model [70] has been illustrated in Eqs. 3–10.

$$f_c = \frac{f'_{cc}.x.r}{r - 1 + x^r} \tag{3}$$

$$x = \frac{\in_c}{\in_{cc}} \tag{4}$$

$$\in_{cc} = \in_{co}.\left[1 + 5.\left(\frac{f'_{cc}}{f'_{co}} - 1\right)\right] \tag{5}$$

where f_c = compressive strength at $\in_c$

where f'_{cc}= compressive strength of confined concrete

where $\in_c$= longitudinal compressive concrete strain

where $\in_{cc}$= longitudinal compressive concrete strain at ultimate strength

where $\in_{co}$= longitudinal compressive concrete strain at ultimate strength of unconfined concrete

where f'_{co}= compressive strength of unconfined concrete

$$r = \frac{E_C}{E_C - E_{\text{sec}}} \tag{6}$$

where E_c= Modulus of elasticity of concrete

$$E_{\text{sec}} = \frac{f'_{cc}}{\in_{cc}} \tag{7}$$

$$f'_{cc} = f'_{co}(-1.254 + 2.254.\sqrt{1 + \frac{7.94.f'_l}{f'_{co}}} - 2.\frac{f'_l}{f'_{co}} \tag{8}$$

$$f_l^{'} = \frac{1}{2}.K_e.\rho_s.f_y \tag{9}$$

$$K_e = \frac{(1 - \frac{S^{'}}{2.d_s})^2}{1 - \rho_{cc}} \tag{10}$$

Where $S^{'}$= the spacing of transverse reinforcement
Where d_s= the height of transverse reinforcement
Where ρ_{cc}= ratio of area of longitudinal reinforcement to area of core of section
Where ρ_s= ratio of the volume of transverse confining steel to the volume of confined concrete core
Where f_y= yield strength of transverse steel

For ECC both (compression and tension) behaviors must be considered to simulate the actual response of the composite. For this purpose, Ding et al. [71] model for compressive stress strain curve of ECC. The mathematical framework for this model has been explained in Eqs. 11–15.

$$\frac{\sigma}{f_c} = 1.327\left(\frac{\varepsilon}{\varepsilon_O}\right) - 0.327\left(\frac{\varepsilon}{\varepsilon_O}\right)^2 0 \le \frac{\varepsilon}{\varepsilon_O} \le 1 \tag{11}$$

$$\frac{\sigma}{f_c} = -0.748\left(\frac{\varepsilon}{\varepsilon_O}\right) + 1.748\frac{\varepsilon}{\varepsilon_O} > 1 \tag{12}$$

Where σ= Compressive stress of ECC at strain ε.
Where f_c= Compressive strength of ECC
The next step is to find the inflection point by simultaneously solving the Eqs. 13 and 14

$$\frac{\sigma}{f_c} = 0.745 - 0.00341 f_c \tag{13}$$

$$\frac{\varepsilon}{\varepsilon_O} = 1.341 + 0.00465 f_c \tag{14}$$

Finally, use Eq. 15 to find the post inflection point curve

$$\frac{\sigma}{f_c} = -0.0465\left(\frac{\varepsilon}{\varepsilon_O}\right) - 0.0032 f_c + 0.807 \tag{15}$$

Similarly, Quan et al. [72] model for tension are used to develop a material level constitutive model as shown in Fig. 6. The method provide two coordinate points of tensile stress strain curve, using those the complete constitutive model is obtained in terms of bi linear stress strain curve as depicted by Fig. 6. These two points include the yield point stress (σ_{tc}) and strain (ε_{tc}), and the ultimate point stress (σ_{tu})and strain (ε_{tu}). The mathematical formulae for calculating these points are shown in Eqs. 16–19

$$\frac{\sigma_{tc}}{\sigma_{tm}} = 0.7.\ln\left(\frac{L_f.V_f}{d_f}\right) - 0.16 \tag{16}$$

Where σ_{tm}= Tensile strength of matrix
Where L_f= Length of fiber used
Where V_f= Volume of fiber used
Where d_f= Diameter of fiber used

$$\frac{\sigma_{tu}}{\sigma_{tm}} = 1.33.\ln\left(\frac{L_f.V_f}{d_f}\right) - 1.18 \tag{17}$$

$$\varepsilon_{tu} = 6.6.\ln\left(\frac{L_f.V_f}{d_f}\right) - 10.7 \tag{18}$$

$$\varepsilon_{tc} = \frac{\sigma_{tc}}{V_f.E_f + (1 - V_f)E_m} \tag{19}$$

Where E_f= Elastic modulus of fiber used
Where E_m= Elastic modulus of matrix

The elastic modulus of the composite is calculated directly from the stress-strain curve [27]. Whereas Poisson's ratio and unit weight are calculated using JSCE guidelines [26] as mentioned in Table 3. The material's idealized stress strain curves were included in the FEM along with the performance level in terms of IO, LS, and CP as shown in Fig. 6.

4.2. Selection of ground motions

The site is located in Karachi, Sindh, Pakistan. The site class is D as per geotechnical reports, and the seismic design coefficients are found to be $S_s = 0.94$; $S_1 = 0.3$ [37] as mentioned in Table 5. Other parameters required for the selection of ground motion are taken from published literature and are mentioned in Table 9.

The ground motions are obtained from the PEER website using the above parametric criteria. Three ground motions were selected for the dynamic analysis namely (earthquake name/station name/direction) Kern County/LA-Hollywood Stor FF/90, Northridge/LB - City Hall/90, and Chi-Chi Taiwan/CHY027/90. The spectral matching was performed [74] in the time domain to scale the selected ground motion according to our design spectrum of the site [38], so that lateral loadings are within the limit for which the structure is to be designed. The key seismic parameters for the ground motions are shown in Table 10. The time histories, original spectrum, and matched spectrum are shown in Table 11 for each ground motion.

5. Results and discussion

5.1. Nonlinear static (Pushover) analysis

The lateral performance of the structure is evaluated by pushing it statically up to a certain displacement, known as roof displacement, to calculate its base shear capacity. Pushover analysis helps to calculate any structure's base shear capacity in the form of static pushover curves. The pushover curve also allows to calculate the complete lateral response of the structure. As the purpose of this study is to compare the material behavior at the structural level for both reinforced ECC and RC, static pushover curves are determined for all 3 models in the first mode pattern along the x and y axis respectively as shown in Fig. 7. The hinge states of all the models are also monitored at the last step when displacement is the maximum which ensures maximum number of hinges have been formed.

Fig. 7 shows how ECC performs significantly better as compared to RC under lateral loading. The curves in Fig. 7 clearly verify that the ultimate load bearing capacity of ECC members is double as compared to RC. Furthermore, due to strain hardening behavior of ECC, the ECC models do not show a sudden drop in the load bearing capacity. Even though, due to reduced cross-sections, stiffness is decreased but still, the base shear capacity is significantly better as compared to RC. This verifies the economic aspects of ECC without any compromise on the capacity of the structure. Alongside, the hinge results confirmed that the plastic hinges formed are way less (almost 7 times less) in ECC structures as compared to RC due to the inherent ductility of ECC as shown in Figs. 8 and 9.

5.2. Results of nonlinear time history analysis (NLTHA)

For NLTHA, a sample ground motion is needed that can be applied to the structure. The ground motion used is as described in Section 4.2 and is applied to the structure after being spectrally matched to the design response spectrum. This analysis is performed on all 3 nonlinear models and the comparison of their responses is summarized in Figs. 10 and 11.

The results showed an increase in story drift and displacement in ECC due to its lower stiffness. The drift and displacement are still within the limits prescribed by the codes [6]. As ECC can sustain much higher strains the higher displacements (as validated by pushover curves in Fig. 7.) can also be considered safe as far as they are acceptable considering serviceability requirements. This fact can also be validated by pushover curves that ECC structures yield at much higher drifts as compared to RC, as shown in Fig. 8. However, the overturning moments and storey shears are reduced in the case of ECC and are much lesser for reduced cross-section ECC. This is due to the lower unit weight of ECC, which reduces the overall seismic weight of the structure [6]. Fig. 12 and Fig. 13 show the plastic hinges formed in the structures in the case of DBE-level and MCE-level excitations respectively. The results clearly show that plastic hinge formation is minimum for ECC structures due to the greater amount of ductility. This clearly shows that the damages produced in the members of ECC are way lesser as compared to RC for a similar level of ground motion.

6. Comparative cost analysis

Considering the material constituents, the per unit volume cost of ECC is higher than that of conventional concrete. However, this study revealed that the cross sections and amount of steel needed for similar structures are quite less for ECC. This led to performing a

Table 9
Site hazard parameters.

Selection Criteria	Values	Reason
Fault Type	Reverse/Oblique	The closest fault and most contributing to Karachi and hence site is Nagar-Parkar Fault which is a reverse fault [49]
Magnitude	6.4–8.2	On average Nagar-Parkar fault causes earthquakes of this magnitude range [73]
R_{JB} (Km)	40–150 Km	Distance of Nagar Parkar fault to Karachi city
R_{RUP} (Km)	40–150 Km	Distance of Nagar Parkar fault to Karachi city
V_{S30} (m/s)	180–360 m/s	Corresponding to Class D [38]
D5–95 (sec)	30–50 sec	To ensure number of cycles for peak response
Pulse	No Pulse-like Records	Not Applicable

Table 10
Key parameters for the selected ground motions.

Parameter	Northridge	Kern County	Chi-Chi Taiwan
Magnitude	6.69	7.36	7.62
Station	LB - City Hall	LA-Hollywood Stor FF	CHY027
Mechanism R_{JB} (Km) R_{RUP} (Km)	Reverse 53.94 57.68	Reverse 114.62 117.75	Reverse Oblique 41.99 41.99

Table 11
The ground motions with their matched and original spectra.

Ground Motion	Matched Spectrum
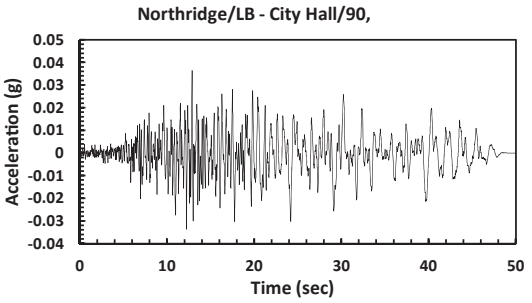	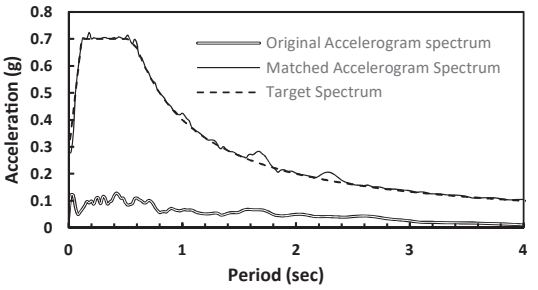
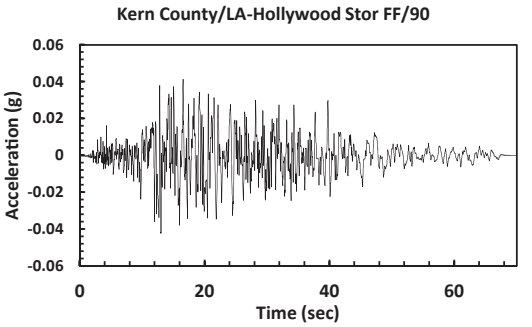	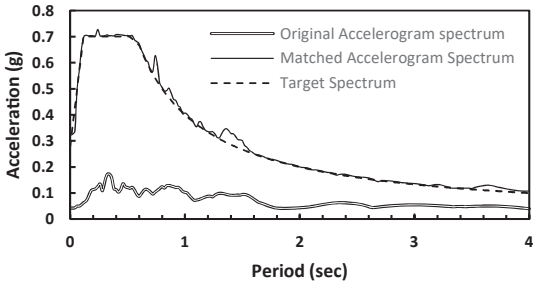
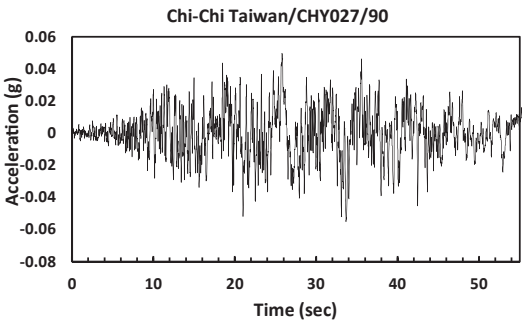	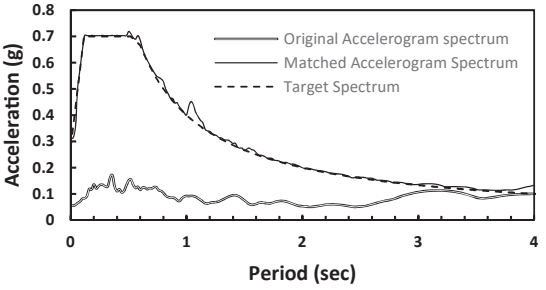

detailed material cost estimation of both structures. For this purpose, a structure with conventional concrete and ECC with reduced cross sections is used. ECC with the same cross-sections is neglected for cost estimation because such large cross-sections of ECC are impractical to be used. The details of the bill of quantities (BOQs) are summarized in Table 12.

The material cost of BOQs summarized in Table 13 is calculated using Pakistan's local market rates for 2021. The conversion rate used is 1 USD = 172.5 PKR as per November 2021. For concrete, the rate is directly estimated from the volume. However, for ECC rate is calculated using the constituent's amounts and their discrete rates. The summary of the cost calculated is shown in Table 13.

The cost estimation as shown in Table 13 shows an 11.9% reduction in the overall material cost of the structure. Additionally, it has been proven that the serviceability and maintenance cost of ECC is also way less due to its self-healing property [75–77]. In this way, the ECC structures apart from being safe, can be cost effective in both the long and short term as compared to RC.

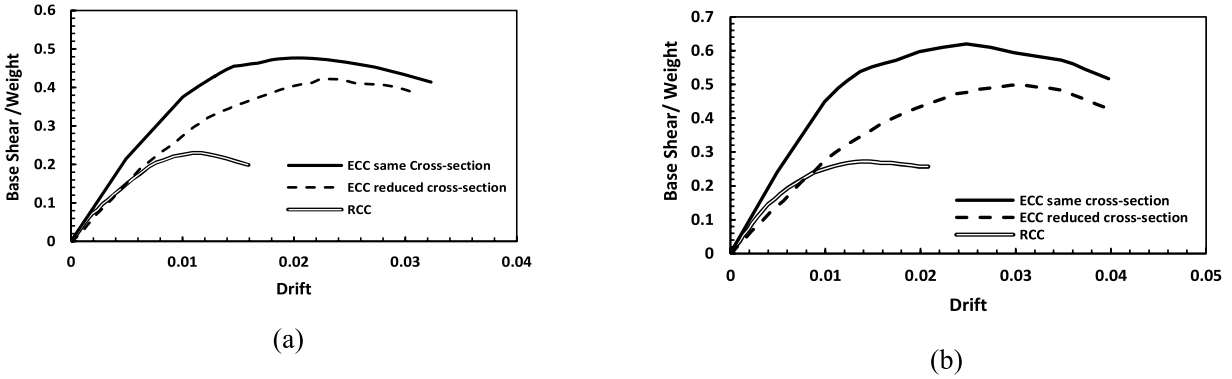

Fig. 7. The normalized static pushover curves (a) along X-axis (b) Y-axis.

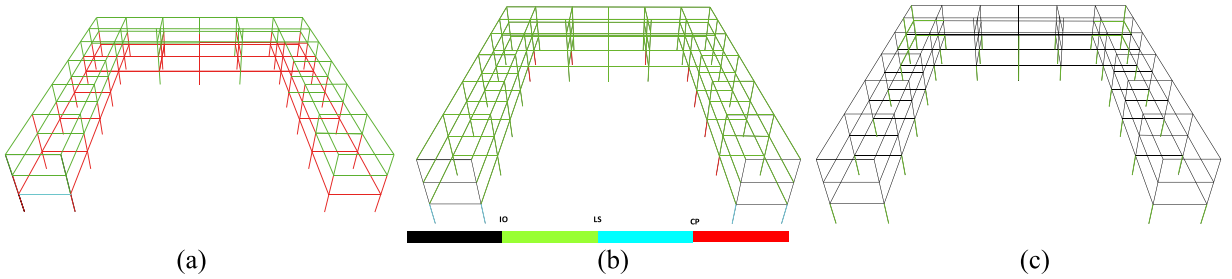

Fig. 8. The hinge states (performance levels) at the last step of pushover analysis about Y axis (roof drift = 3%). (a) RC (b) ECC Reduced Cross-sections (c) ECC same Cross-sections.

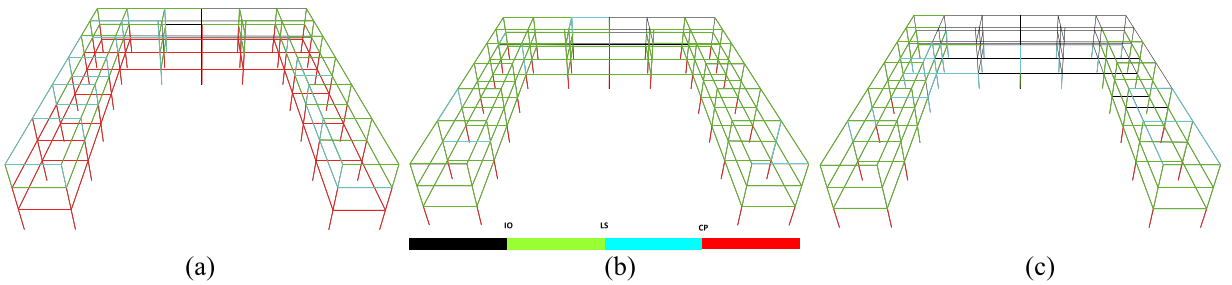

Fig. 9. The hinge states (performance levels) at the last step of pushover analysis about X axis (roof drift = 2.2%). (a) RC (b) ECC Reduced Cross-sections (c) ECC same Cross-sections.

7. Conclusions and recommendations

This research was able to conduct a comprehensive seismic assessment of the long-span ECC structure. For the very first time, both linear and nonlinear FEA models of ECC on the structural scale were developed considering a material level constitutive model. A complete structural design and nonlinear analyses of ECC structures and their comparison with RC structures were performed, and the following conclusions were made:

- Due to the lower unit weight of ECC, the design actions for structural members were approximately reduced by 25% because of the reduction in dead and seismic loads.
- Due to the better tensile capacity of ECC, the cross sectional sizes of the structural members were reduced by 25%, making ECC a good alternative to RC in the case of long-span structures. This observation indicates the potential of ECC for long-span structural applications.
- The structural design performed using JSCE guidelines showed an over 30% reduction of longitudinal steel in flexural members and about 15% reduction in longitudinal steel in compression members. Alongside, theoretically, the shear reinforcement requirement throughout the structure was eliminated, due to additional shear capacity provided by the fibers.

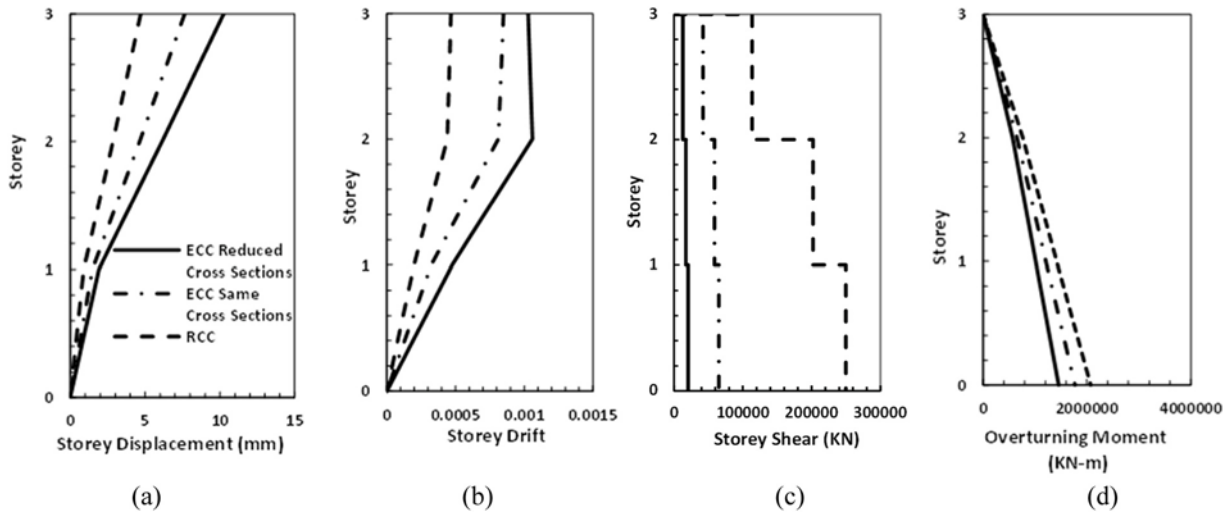

Fig. 10. MCE level storey level responses against Kern County/LA-Hollywood Stor FF/90 (a) storey displacement (b) storey drift (c) storey shear (d) overturning moment.

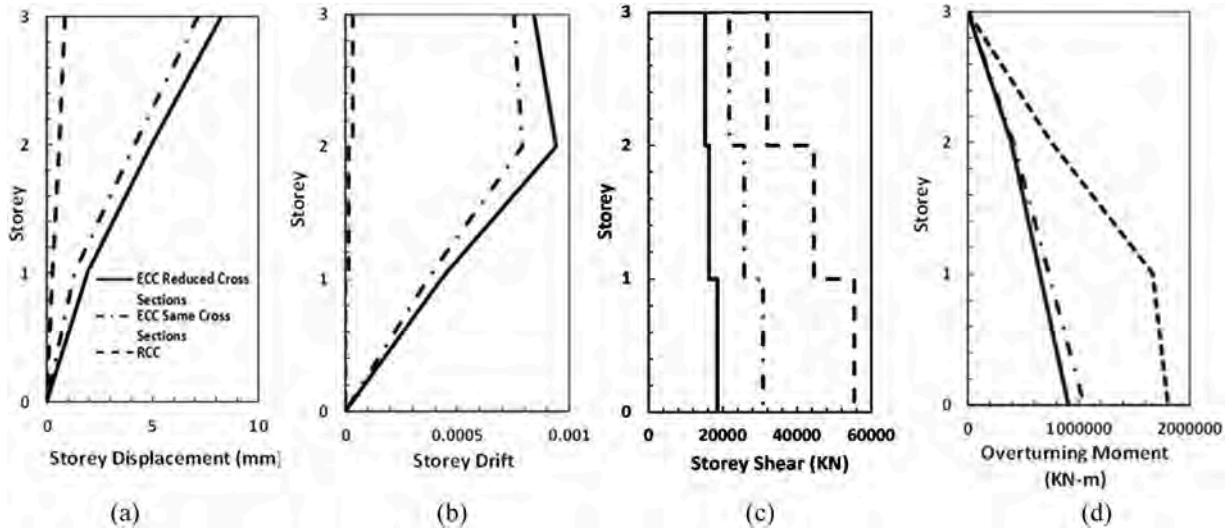

Fig. 11. DBE level storey level responses against Kern County/LA-Hollywood Stor FF/90 (a) storey displacement (b) storey drift (c) storey shear (d) overturning moment.

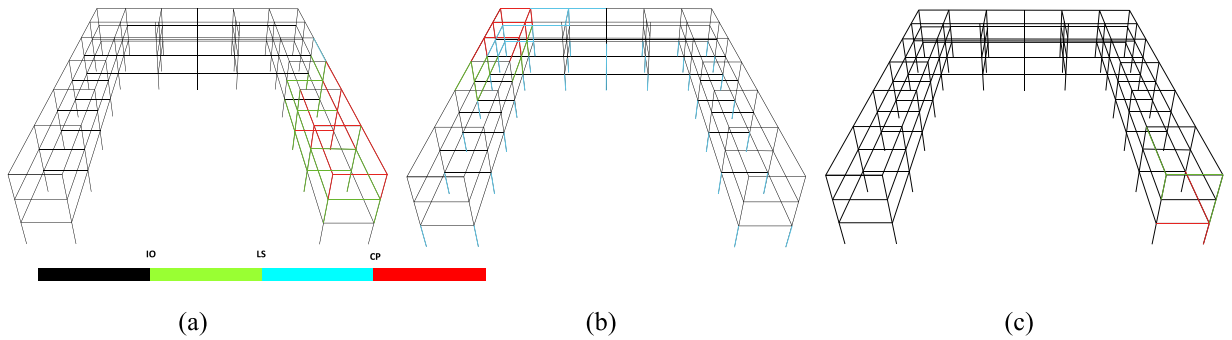

Fig. 12. The hinge states (performance levels) of NLTHA at DBE level against Kern County/LA-Hollywood Stor FF/90 (a) RC (b) ECC reduced cross sections (c) ECC same cross-section.

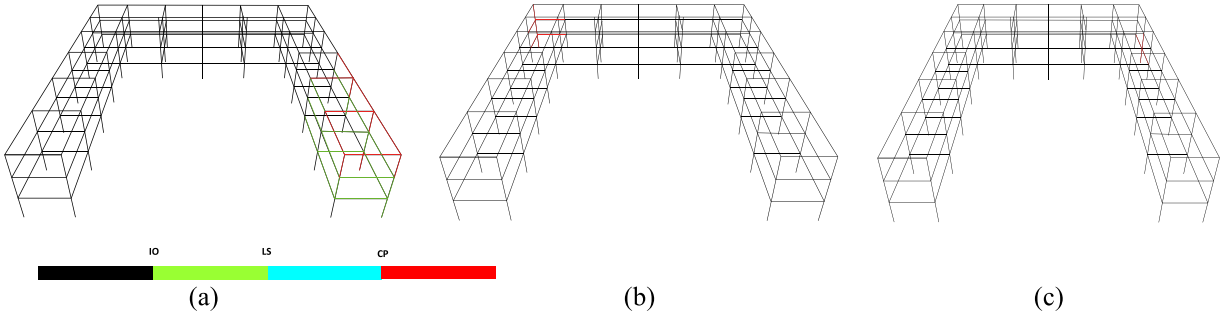

Fig. 13. The hinge states (performance levels) of NLTHA at MCE level against Kern County/LA-Hollywood Stor FF/90 (a) RC (b) ECC reduced cross sections (c) ECC same cross-section.

Table 12
BOQs of RC and ECC.

BOQs of RC			
Item		Quantity	Units
Volume of Concrete	Flexure members	1654	m^3
	Column	254	m^3
	Total	1908	m^3
Rebars weight	Flexural members	115968	Kg
	Column	41998	Kg
	Total	157966	Kg
BOQs of ECC			
Item		Quantity	Units
Volume of Concrete	Flexural members	1274	m^3
	Column	200	m^3
	Total	1474	m^3
Rebar's weight	Flexural members	73342	Kg
	Column	25000	Kg
	Total	98342	Kg
PVA fibers	Total	2852	Kg

Table 13
Summary of cost.

Material	**Unit cost**		**Price**
Concrete	USD 46.37/m^3		98,550
Steel rebars	USD 1.12 /Kg		178,000
Total Price	**USD 276,550**		
Ingredient	**Quantities**	**Unit price**	**Total Price**
	Kgs	**PKR**	
Cement	965454	3.48/- per 50 kg	67,130
Fly-ash	382159	0.035/- per kg	13,275
PVA fibers	38350	0.70/- per Kg	26,700
Fine Sand	885000	0.0058/- per kg	5100
Superplasticizer	5792	3.77/- per kg	21,500
steel	98342	1.11/- per kg	109,000
Total Price	**USD 243,480**		

- The nonlinear analyses clearly showed better seismic performance (in terms of local and global seismic demands, structural damage, and ductile behavior) of ECC due to its increased capacity and lower inertial forces being developed within the structure.
- The static nonlinear analysis showed that the significantly damaged elements (plastic hinges above CP) in the ECC structure were around 12, while at the similar drift in the RC structure were about 79. This clearly shows that ECCs perform better as compared to RC under lateral loadings. Similar sorts of results were obtained for non-linear dynamic analysis as well.
- However, due to the lower material stiffness of ECC, the displacements and drifts calculated using linear and nonlinear analyses were higher as compared to RC. But still, the values were within the limits prescribed by IBC 2021.
- The detailed cost estimation comparison showed an 11.9% reduction in the material cost of the structure, which endorses ECC's commercial implementation potential.
- The results clearly demonstrate the effectiveness of ECC to be used at full structural scale as a cost effective solution for sustainable and resilient long span structures.

It is recommended that future research should be carried out to find actual parameters to avoid assumptions in the design process. The design procedure and certain assumptions, being on the safer side, adopted in this paper give conservative designs. These conservative approaches are due to the unavailability of authentic numeric data for ECC. For example, stiffness modifiers and damping ratio for ECC should be investigated for further accuracy in design and analysis procedures. Alongside this, the structural response of ECC in other special structures should be investigated.

CRediT authorship contribution statement

Rao Arsalan Khushnood: Conceptualization, Data curation, Project administration, Supervision, Validation, Writing – review & editing. **Muhammad Umer Basit:** Formal analysis, Software, Validation. **Fawad Ahmed Najam:** Conceptualization, Investigation, Project administration, Software, Supervision, Writing – review & editing. **Shahzeb Memon:** Data curation, Formal analysis, Methodology, Software. **Touqeer Ahmed:** Data curation, Investigation, Resources, Validation, Visualization, Writing – original draft. **Sikandar Ali Ali Khokhar:** Conceptualization, Data curation, Formal analysis, Methodology, Writing – original draft.

Declaration of Competing Interest

The authors declared no potential conflicts of interest with respect to the research, authorship, and/or publication of this article.

Data availability

Data will be made available on request.

Acknowledgements

The authors would like to express their gratitude to Eman Bilal for providing architectural drawings for the case study structure.

References

[1] C. Jiansinlapadamrong, K. Park, J. Hooper, M. Asce, and S.-H. Chao, Seismic Design and Performance Evaluation of Long-Span Special Truss Moment Frames, 2019, doi: 10.1061/(ASCE)ST.1943.
[2] P. Fuentes, S. HuertaIslamic domes of crossed-arches: origin, geometry and structural behavior, in Arch' 10 6th International Conference on Arch Bridges , 2010, 346–353.
[3] S. Rodriguez, Design of Long Span Concrete Box Girder Bridges: Challenges and Solutions, 2004.
[4] C. Wang, Y. Shen, R. Yang, Z. Wen, Ductility and ultimate capacity of prestressed steel reinforced concrete beams, Math. Probl. Eng. vol. 2017 (2017), https://doi.org/10.1155/2017/1467940.
[5] H. Kaur, J. Singh, A review on external prestressing in concrete, Int. Res. J. Eng. Technol. (2008) 1801 ([Online]. Available: www.irjet.net).
[6] International Code Council, *International Building Code*, 2021st ed. 2021.
[7] M.H. Chey, J.G. Chase, J.B. Mander, A.J. Carr, Innovative seismic retrofitting strategy of added stories isolation system, Front. Archit. Civ. Eng. China vol. 7 (1) (Mar. 2013) 13–23, https://doi.org/10.1007/s11709-013-0195-9.
[8] H.L. Hsu, H. Halim, Improving seismic performance of framed structures with steel curved dampers, Eng. Struct. vol. 130 (2017) 99–111, https://doi.org/10.1016/j.engstruct.2016.09.063.
[9] Arnon. Bentur and Sidney, Mindess. Fibre Reinforced Cementitious Composites, Taylor & Francis, 2007.
[10] S. Guler, Z.F. Akbulut, Residual strength and toughness properties of 3D, 4D and 5D steel fiber-reinforced concrete exposed to high temperatures, Constr. Build. Mater. vol. 327 (2022) 126945, https://doi.org/10.1016/j.conbuildmat.2022.126945.
[11] S. Guler, Z.F. Akbulut, The effects of single and hybrid polypropylene fibers on the workability and residual strength properties of concrete road pavements against freeze–thaw cycles, Arab J. Sci. Eng. (2023), https://doi.org/10.1007/s13369-023-07879-6.
[12] S. Guler, Z.Funda Akbulut, Workability & mechanical properties of the single and hybrid basalt fiber reinforced volcanic ash-based cement mortars after freeze–thaw cycles, Structures vol. 48 (2023) 1537–1547, https://doi.org/10.1016/j.istruc.2023.01.062.
[13] M. Chen, Y. Wang, T. Zhang, M. Zhang, Behaviour of structural engineered cementitious composites under dynamic tensile loading and elevated temperatures, Eng. Struct. vol. 280 (2023) 115739, https://doi.org/10.1016/j.engstruct.2023.115739.
[14] J.-Z. Tong, Y.-L. Chen, Q.-H. Li, S.-L. Xu, T. Zeng, W. Gao, Experimental study on flexural performance of steel-UHTCC composite bridge decks considering different shear connection degrees, Eng. Struct. vol. 281 (2023) 115738, https://doi.org/10.1016/j.engstruct.2023.115738.
[15] H. Zhou, J. Wu, X. Wang, Y. Chen, X. Du, S. Yu, Performance of engineered cementitious composite (ECC) monolithic and composite slabs subjected to near-field blast, Eng. Struct. vol. 279 (2023) 115561, https://doi.org/10.1016/j.engstruct.2022.115561.
[16] V.C. Li, From Micromechanics to Structural Engineering - the design of cementitous composites for civil engineering applications, JSCE J. Struct. Mech. Earthq. Eng. (1993) 37–48.
[17] V.C. Li, S. Wang, C. Wu, Tensile strain-hardening behavior of polyvinyl alcohol engineered cementitious composite (PVA-ECC), Acids Mater. J. (2001) 483–492.
[18] V.C. Li, On Engineered Cementitious Composites (ECC) A Review of the Material and Its Applications, 2003. [Online]. Available: https://www.researchgate.net/publication/237783722.
[19] J. Tian, et al., Experimental study and mechanics model of ECC-to-concrete bond interface under tensile loading, Compos Struct. vol. 285 (Apr. 2022) 115203, https://doi.org/10.1016/j.compstruct.2022.115203.
[20] C.-C. Hung, H.-J. Hsiao, Y. Shao, C.-H. Yen, A comparative study on the seismic performance of RC beam-column joints retrofitted by ECC, FRP, and concrete jacketing methods, J. Build. Eng. vol. 64 (2023) 105691, https://doi.org/10.1016/j.jobe.2022.105691.
[21] N. Zhang, Q. Gu, Y. Dong, J. Qian, Y. Zheng, Seismic performance of bridges with ECC-reinforced piers, Soil Dyn. Earthq. Eng. vol. 146 (2021) 106753, https://doi.org/10.1016/j.soildyn.2021.106753.
[22] L. Xu, J. Pan, J. Cai, Seismic performance of precast RC and RC/ECC composite columns with grouted sleeve connections, Eng. Struct. vol. 188 (2019) 104–110, https://doi.org/10.1016/j.engstruct.2019.03.022.
[23] M.S. Khan, Seismic performance of deficient RC frames retrofitted with SMA-reinforced ECC column jacketing, Innov. Infrastruct. Solut. vol. 6 (3) (2021) 157, https://doi.org/10.1007/s41062-021-00529-6.
[24] F.A. Khan, et al., Comparative seismic performance assessment of RC and RC/ECC hybrid frame structures: a shake table study, Innov. Infrastruct. Solut. vol. 7 (1) (2022) 94, https://doi.org/10.1007/s41062-021-00692-w.

[25] C. Wu, Z. Pan, C. Jin, S. Meng, Evaluation of deformation-based seismic performance of RECC frames based on IDA method, Eng. Struct. vol. 211 (2020) 110499, https://doi.org/10.1016/j.engstruct.2020.110499.
[26] V.C. Li, T. Hashida, Engineering ductile fracture in brittle-matrix composites, J. Mater. Sci. Lett. vol. 12 (12) (1993) 898–901, https://doi.org/10.1007/BF00455611.
[27] T. Kanda, V.C. Li, Practical design criteria for saturated pseudo strain hardening behavior in ECC, J. Adv. Concr. Technol. vol. 4 (1) (2006) 59–72, https://doi.org/10.3151/jact.4.59.
[28] V.C. Li, Integrated structures and materials design, Mater. Struct. /Mater. Et. Constr. vol. 40 (4) (May 2007) 387–396, https://doi.org/10.1617/s11527-006-9146-4.
[29] X. Li, J. Wang, Y. Bao, G. Chen, Cyclic behavior of damaged reinforced concrete columns repaired with high-performance fiber-reinforced cementitious composite, Eng. Struct. vol. 136 (2017) 26–35, https://doi.org/10.1016/j.engstruct.2017.01.015.
[30] H. Fukuyama, Application of high performance fiber reinforced cementitious composites for damage mitigation of building structures case study on damage mitigation of RC buildings with soft first story, J. Adv. Concr. Technol. (2006) 35–44.
[31] M. Maalej and V.C. Li, FLEXURAL/TENSILE-STRENGTH RATIO IN ENGINEERED CEMENTITIOUS COMPOSITES.
[32] M.M. Szerszen, A. Szwed, V.C. LiFlexural Response of Reinforced Beam with High Ductility Concrete Material, in Int. Symp Brittle Matrix Compos. 8 , 2006, 263–274.
[33] Y. Ding, K.-Q. Yu, J. Yu, S. Xu, Structural behaviors of ultra-high performance engineered cementitious composites (UHP-ECC) beams subjected to bending-experimental study, Constr. Build. Mater. vol. 177 (2018) 102–115, https://doi.org/10.1016/j.conbuildmat.2018.05.122.
[34] H.-S. Hu, Z.-J. Yang, L. Xu, Y.-X. Zhang, Y.-C. Gao, Axial compressive behavior of square concrete-filled steel tube columns with high-strength steel fiber-reinforced concrete, Eng. Struct. vol. 285 (2023) 116047, https://doi.org/10.1016/j.engstruct.2023.116047.
[35] H. Fukuyama, Y. Matsuzaki, Y. Sato, M. Iso, H. SuwadaStructural Performance of Engineered Cementitious Composite Elements, Composite and Hybrid Structures 6th ASCCS International Conference on Steel-Concrete Composite Structures , 2000, 969–976.
[36] B.Gustavo Parra-Montesinos and J.K. Wight, SEISMIC RESPONSE OF EXTERIOR RC COLUMN-TO-STEEL BEAM CONNECTIONS, 2000.
[37] S. Qudah, M. Maalej, Application of engineered cementitious composites (ECC) in interior beam-column connections for enhanced seismic resistance, Eng. Struct. vol. 69 (2014) 235–245, https://doi.org/10.1016/j.engstruct.2014.03.026.
[38] S.H. Said, H. Abdul Razak, Structural behavior of RC engineered cementitious composite (ECC) exterior beam-column joints under reversed cyclic loading, Constr. Build. Mater. vol. 107 (2016) 226–234, https://doi.org/10.1016/j.conbuildmat.2016.01.001.
[39] F. Hosseini, B. Gencturk, H. Aryan, G. Cadaval, Seismic behavior of 3-D ECC beam-column connections subjected to bidirectional bending and torsion, Eng. Struct. vol. 172 (2018) 751–763, https://doi.org/10.1016/j.engstruct.2018.06.054.
[40] X. Chen, Z. Xiong, Y. Zhuge, Y. Liu, K. Cheng, W. Fan, Numerical analysis of compressive behavior of pre-damaged concrete columns strengthened with textile-reinforced ECC, Case Stud. Constr. Mater. vol. 18 (2023) e02198, https://doi.org/10.1016/j.cscm.2023.e02198.
[41] C. Zhang, L. Wu, M. Elchalakani, J. Cai, Cyclic loading test for reinforced concrete columns strengthened with high-strength engineered cementitious composite jacket, Eng. Struct. vol. 278 (2023) 115571, https://doi.org/10.1016/j.engstruct.2022.115571.
[42] J.-J. Zeng, et al., Strengthening RC square columns with UHP-ECC section curvilinearization and FRP confinement: concept and axial compression tests, Eng. Struct. vol. 280 (Apr. 2023) 115666, https://doi.org/10.1016/j.engstruct.2023.115666.
[43] C.-C. Hung, Y.-S. Chen, Innovative ECC jacketing for retrofitting shear-deficient RC members, Constr. Build. Mater. vol. 111 (2016) 408–418, https://doi.org/10.1016/j.conbuildmat.2016.02.077.
[44] B. Dadmand, M. Pourbaba, R. Riahi, Experimental and numerical investigation of different types of jacketing effect on retrofitting RC short columns using ECC concrete, Period. Polytech. Civ. Eng. (2022), https://doi.org/10.3311/PPci.19114.
[45] Y. Zhou, X. Wang, F. Yuan, B. Hu, Z. Zhu, Seismic retrofitting of coastal structural columns with steel bars locally corroded to fracture using sprayed ECC overlays and FRP jackets, Compos Struct. vol. 307 (2023) 116670, https://doi.org/10.1016/j.compstruct.2023.116670.
[46] S.A. Khokhar, T. Ahmed, R.A. Khushnood, S.M. Ali, Shahnawaz, A predictive mimicker of fracture behavior in fiber reinforced concrete using machine learning, Materials vol. 14 (24) (2021), https://doi.org/10.3390/ma14247669.
[47] Recommendations for Design and Construction of High Performance Fiber Reinforced Cement Composites with Multiple Fine Cracks (HPFRCC), 2008.
[48] 318-19 Building Code Requirements for Structural Concrete and Commentary. American Concrete Institute, 2019. doi: 10.14359/51716937.
[49] Seismic Evaluation and Retrofit of Existing Buildings. Reston, VA: American Society of Civil Engineers, 2017. doi: 10.1061/9780784414859.
[50] Y. Zhang, S. Zhang, M. Deng, Four-point bending tests of ECC: mechanical response and toughness evaluation, Case Stud. Constr. Mater. vol. 17 (2022) e01573, https://doi.org/10.1016/j.cscm.2022.e01573.
[51] V.C. Li and C.K.Y. Leung, STEADY-STATE AND MULTIPLE CRACKING OF SHORT RANDOM FIBER COMPOSITES.
[52] Z. Lin and V.C. Li, CRACK BRIDGING IN FIBER REINFORCED CEMENTITIOUS COMPOSITES WITH SLIP-HARDENING INTERFACES, 1997.
[53] V.C. Li, H. Stang, H. Krenchel, Micromechanics of crack bridging in fibre-reinforced concrete, Mater. Struct. vol. 26 (8) (1993) 486–494, https://doi.org/10.1007/BF02472808.
[54] V.C. Li, D.K. Mishra, and H.-C. Wu, Matrix Design for Pseudo Strain-Hardening Fiber Reinforced Cementitious Composites.
[55] C.C. Yang, T. Mura, and S.P. Shah, Micromechanical theory and uniaxial tensile tests of fiber reinforced cement composites, 2015. [Online]. Available: http://journals.cambridge.org.
[56] L.N. McCartney, Mechanics of matrix cracking in brittle-matrix fibre-reinforced composites, Proc. R. Soc. Lond. A Math. Phys. Sci. vol. 409 (1837) (1987) 329–350, 10.1098/rspa.1987.0019.
[57] C.K.Y. Leung and A. Member, DESIGN CRITERIA FOR PSEUDODUCTILE FIBER-REINFORCED COMPOSITES.
[58] P. Guo, W. Meng, M. Xu, V.C. Li, Y. Bao, Predicting mechanical properties of high-performance fiber-reinforced cementitious composites by integrating micromechanics and machine learning, Materials vol. 14 (12) (Jun. 2021), https://doi.org/10.3390/ma14123143.
[59] Pakistan Engineering Council, *Building Code of Pakistan*, 2021st ed. 2021.
[60] *Minimum design loads and associated criteria for buildings and other structures*. American Society of Civil Engineers (ASCE), 2017. doi: 10.1061/9780784414248.
[61] V.C. Li *et al.*, On the Shear Behavior of Engineered Cementitious Composites, 1993.
[62] K. Shimizu, T. Kanakubo, T. Kanda, S. Nagai, 2006, , Shear Behavior of PVA-ECC Beams, in Int'l RILEM Workshop HPFRC in Structural Applications443–451G. Fischer, V.C. Li.
[63] Y. Zhang, M. Deng, Z. Dong, Seismic response and shear mechanism of engineered cementitious composite (ECC) short columns, Eng. Struct. vol. 192 (Aug. 2019) 296–304, https://doi.org/10.1016/j.engstruct.2019.05.019.
[64] B. Suryanto, K. Nagai, K. Maekawa, Modeling and analysis of shear-critical ecc members with anisotropic stress and strain fields, J. Adv. Concr. Technol. vol. 8 (2) (Jun. 2010) 239–258, https://doi.org/10.3151/jact.8.239.
[65] V.C. Li, Damage tolerance of engineered cementitious composites, 9th ICF Conf. Fract. (1997) 619–630.
[66] G. Fischer, Li, and Victor C., Influence of Matrix Ductility on Tension-Stiffening Behavior of Steel Reinforced Engineered Cementitious Composites (ECC), *ACI Struct J*, vol. 99, no. 1, doi: 10.14359/11041.
[67] Y.K. Wen, Reliability and performance-based design, Struct. Saf. vol. 23 (2001) ([Online]. Available: www.elsevier.com/locate/strusafe).
[68] I. Computers and Structures, ETABS Nonlinear v9.7.4. 2011.
[69] A.S. of Civil. EngineersAmerican Society of Civil Engineers, and Structural Engineering Institute American Society of Civil Engineers , Seismic Evaluation and Retrofit of Existing Buildings: ASCE/SEI 41-17 , 2017.
[70] J.B. Mander, M.J.N. Priestley, and R. Park, THEORETICAL STRESS-STRAIN MODEL FOR CONFINED CONCRETE.
[71] Y. Ding, K. Yu, W. Mao, Compressive performance of all-grade engineered cementitious composites: experiment and theoretical model, Constr. Build. Mater. vol. 244 (May 2020), https://doi.org/10.1016/j.conbuildmat.2020.118357.

[72] K.-Q. Yu, Z.-D. Lu, J.-G. Dai, S.P. Shah, Direct tensile properties and stress–strain model of UHP-ECC, J. Mater. Civ. Eng. vol. 32 (1) (2020), https://doi.org/10.1061/(asce)mt.1943-5533.0002975.
[73] S. Zaman and P. Warnitchai, Probabilistic Seismic Hazard Maps for Pakistan Teraphan Ornthammarath Regional Integrated Multi-Hazard Early Warning System AIT, Bangkok,Thailand. [Online]. Available: http://www.isc.ac.uk.
[74] J. Hancock *et al.*, AN IMPROVED METHOD OF MATCHING RESPONSE SPECTRA OF RECORDED EARTHQUAKE GROUND MOTION USING WAVELETS, 2006. [Online]. Available: www.worldscientific.com.
[75] M. Li, R. Ranade, L. Kan, and V.C. Li, ON IMPROVING THE INFRASTRUCTURE SERVICE LIFE USING ECC TO MITIGATE REBAR CORROSION.
[76] Y. Yang, M.D. Lepech, E.H. Yang, V.C. Li, Autogenous healing of engineered cementitious composites under wet-dry cycles, Cem. Concr. Res vol. 39 (5) (2009) 382–390, https://doi.org/10.1016/j.cemconres.2009.01.013.
[77] L.-L. Kan, H.S. Shi, A.R. Sakulich, V.C. Li, Self-healing characterization of engineered cementitious composite materials, ACI Mater. J. (2010) 617–624.